DEFORMATION AND FATIGUE BEHAVIOR OF SSME TURBOPUMP BLADE MATERIALS

Walter W. Milligan and Stephen D. Antolovich
Georgia Institute of Technology
Atlanta, Georgia

Directionally solidified and single crystal superalloys which are intended for use as turbopump blade materials are anisotropic, both elastically and plastically. Therefore, isotropic constitutive models must be modified. Several models which are now being developed are based on metallurgical theories of deformation in these types of alloys. However, these theories have not been fully justified, and the temperature and strain regimes over which they may be valid are poorly defined. The objective of this work is to study the deformation behavior of the alloys, in order to determine the validity of these models and to thereby support the ongoing research efforts in solid mechanics.

REFERENCES

1. Milligan, W.W.; and Antolovich, S.D.: Yielding and Deformation Behavior of the Single Crystal Superalloy PWA 1480. Metall. Trans. A., vol. 18, no. 1, Jan. 1987, pp. 85-95.

2. Milligan, W.W., Jr.: Yielding and Deformation Behavior of the Single Crystal Nickel-Base Superalloy PWA 1480. (USAAVSCOM TR-86-C-18, Georgia Institute of Technology; NASA Grant NAG3-503) NASA CR-175100, 1986.

3. Huron, E.S.: High Temperature Monotonic and Cyclic Deformation in a Directionally Solidified Nickel-Base Superalloy. (USAAVSCOM TR-86-C-19, Georgia Institute of Technology; NASA Grant NAG3-503) NASA CR-175101, 1986.

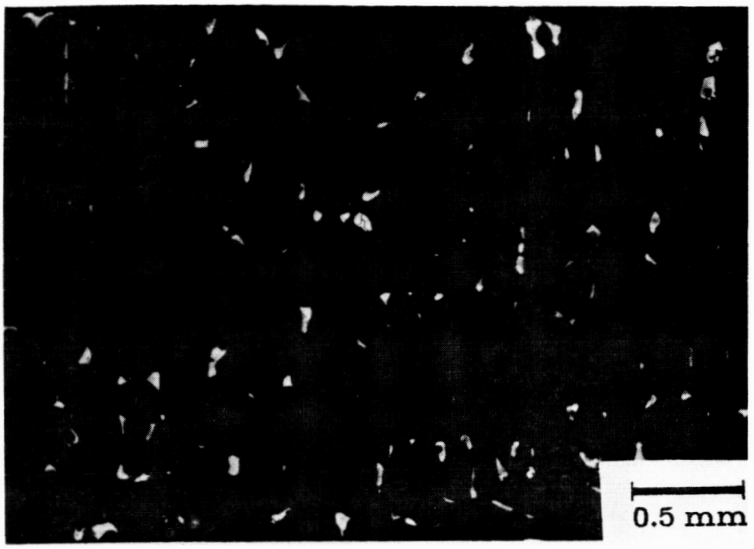

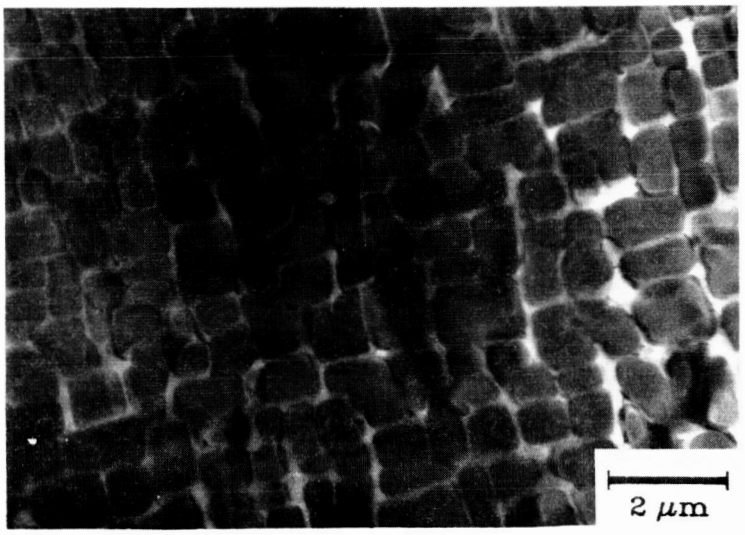

Figure 1. - PWA 1480 initial microstructure.

Classical Plasticity Theory

$$\dot{\epsilon}_t = \frac{\dot{\sigma}}{E} + \dot{\epsilon}_p + \dot{\epsilon}_c$$

Unified Constitutive Theory

$$\dot{\epsilon}_{(in)} = \dot{\epsilon}_t - \frac{\dot{\sigma}}{E} = f^{-1}\left[\frac{\sigma_{ij} - \Omega_{ij}}{K}\right]$$

Figure 2. - Constitutive modeling.

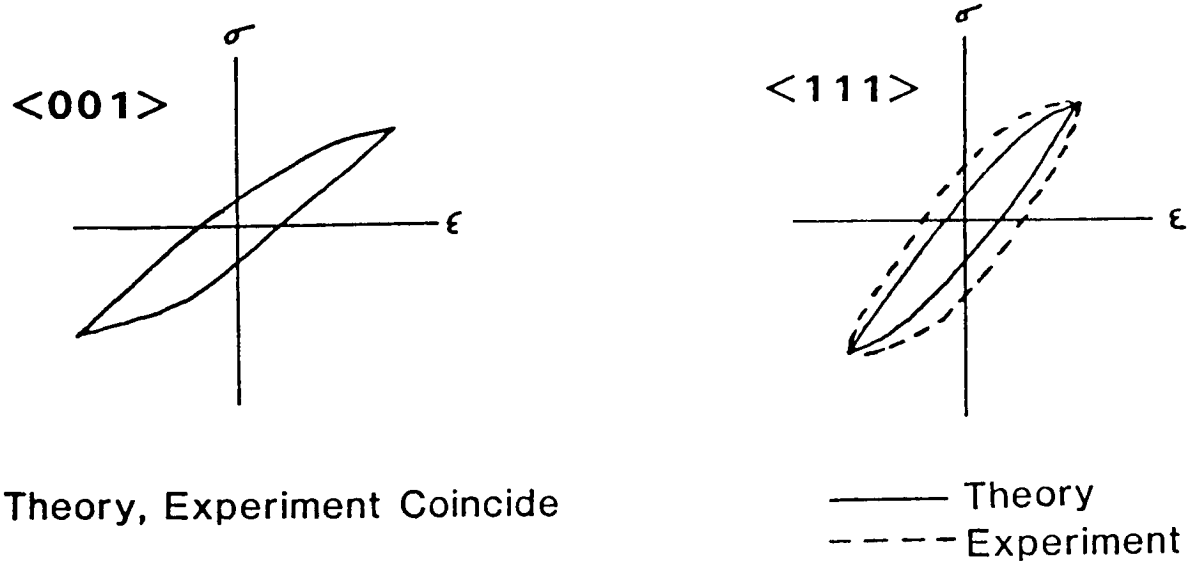

Figure 3. - PWA 1480 at 1600 °F - after K.P. Walker and E. Jordan.

$$\dot{\gamma}_p = \sum_{i=1}^{n} \dot{\gamma}_i \quad ;$$

$$\dot{\gamma}_i = f^{-1}\left[\frac{\underline{\sigma}_i - \underline{\Omega}_i}{K_i}\right]$$

<110>(111)

<112>(111)

<110>(001)

Figure 4. - Unified crystallographic approach.

Crystallographic approach requires physical validation

-Active slip systems

-Cube slip only observed in γ'

-Slip planarity

-Deformation mechanisms

Figure 5.

$$\gamma_o = b\rho_o\lambda \leq 0.006\%$$

γ' must be "overcome" for substantial plasticity

Figure 6. - Deformation mechanisms.

Possibilities:

1. Looping
2. Shearing
3. Climb-assisted Bypass

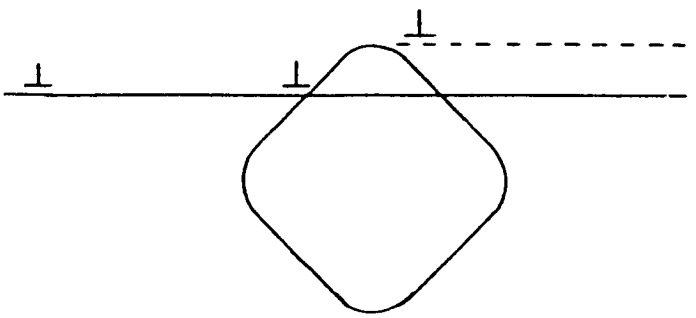

Figure 7.

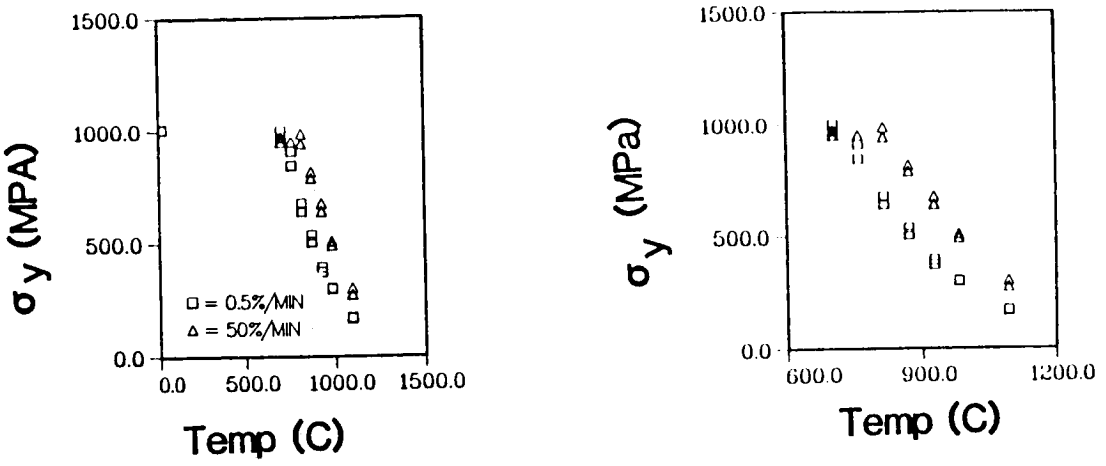

Figure 8. - PWA 1480 yield strength (0.05 percent offset) versus temperature.

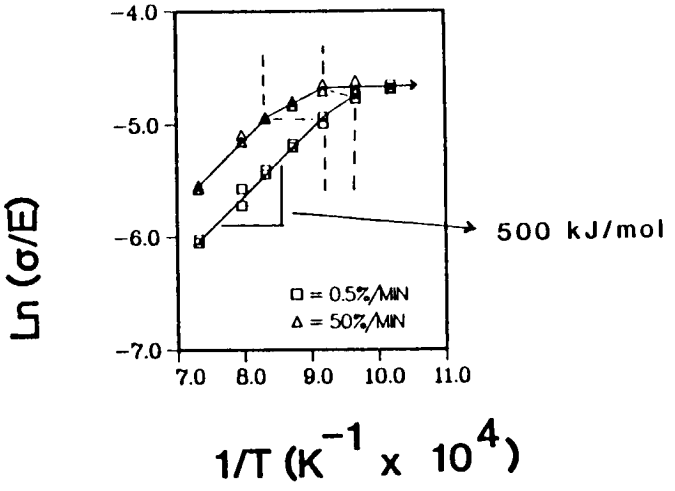

Figure 9. - PWA 1480 modulus normalized yield; strength versus inverse temperature.

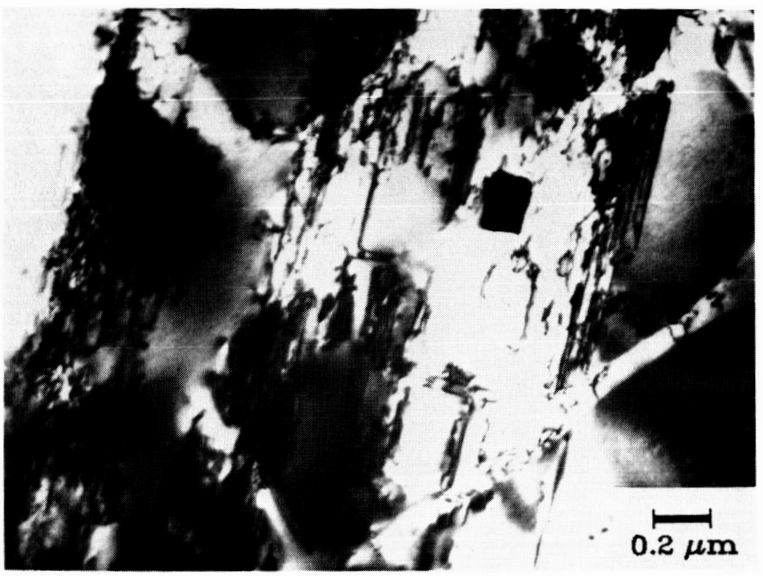

Figure 10. - γ' Shearing by slip bands at low temperatures (0.1 percent ε_p).

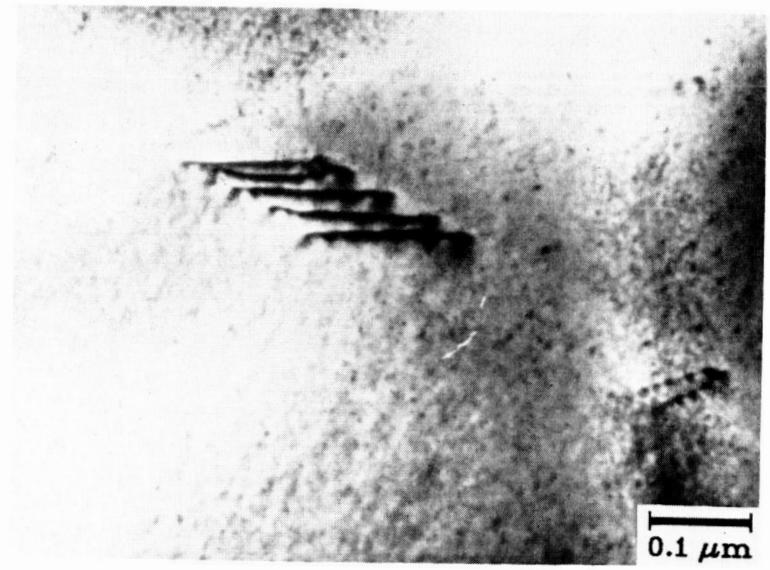

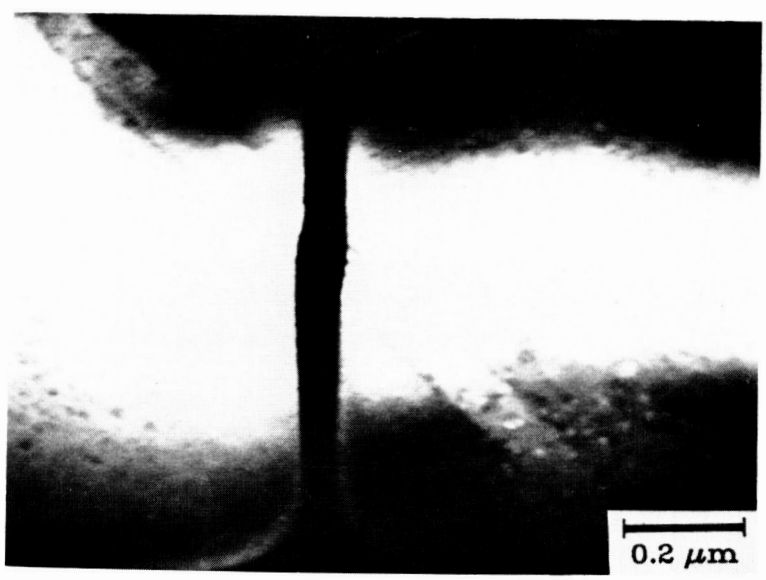

Figure 11. - Shear offsets parallel to $\bar{b}$.

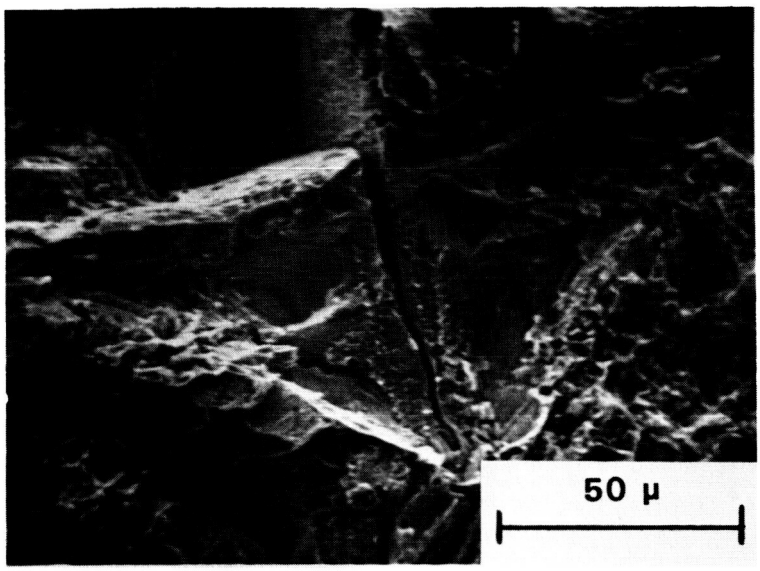

Figure 12. - Typical tensile fracture surface.
(D.S. Mar-M 246 tested at room temperature.)

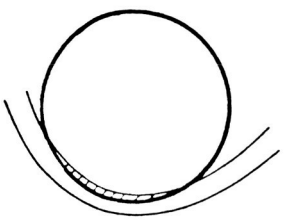

$$(\tau - \tau_p)b + \frac{c}{\Delta x} + \frac{\phi}{r_o} - \gamma = 0$$

$$(\tau - \tau_m)b - \frac{c}{\Delta x} + \frac{\phi}{r_o} = 0$$

$$\tau_c = \frac{\gamma}{2b} - \frac{Gb}{2r_o} + \frac{1}{2}(\tau_m + \tau_p)$$

Figure 13. - Low temperature
(Copley-Kear, Huther-Reppich).

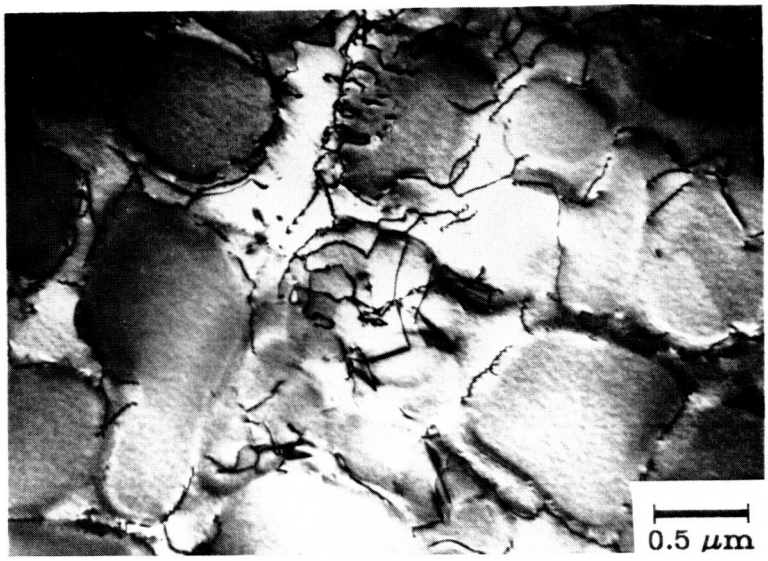

Figure 14. - γ' Bypass at high temperatures (0.3 percent ε_p).

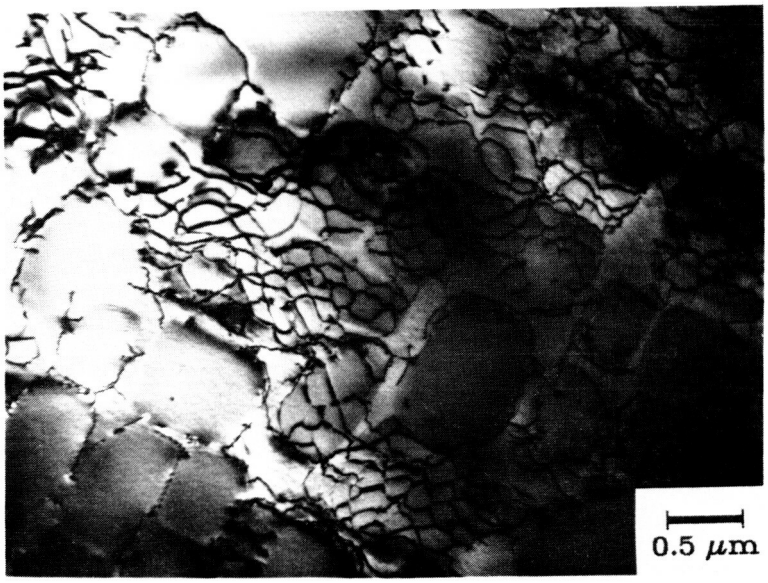

Figure 15. - Interfacial network of dislocations developed at 1093 °C after about 0.25 percent ε_p.

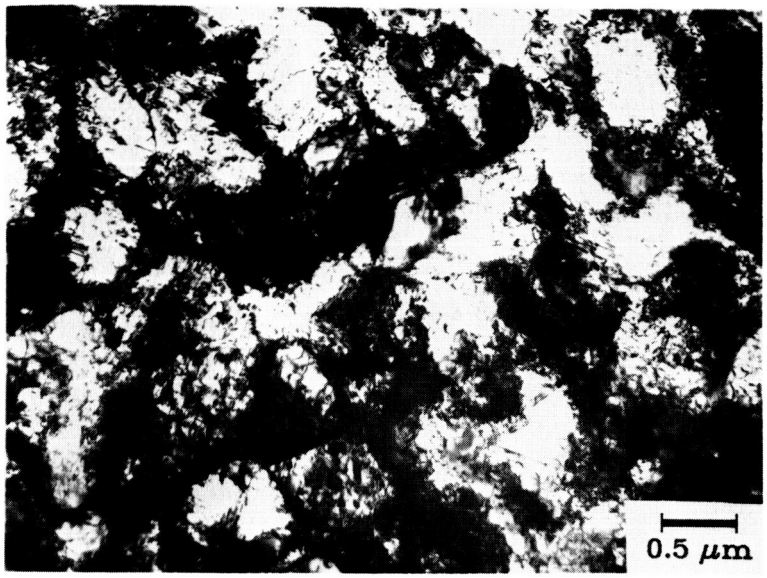

Figure 16. - High dislocation density at failure at 871 °C.

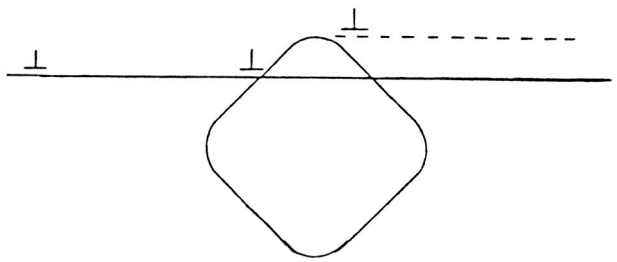

Climb is rate-limiting step

–Controlled by diffusion

$$\tau_c = k_1 Q_D - k_2 T \left| \log(k_3 \dot{\epsilon}) \right|$$

Figure 17. - High temperatures (Brown and Ham, bypass model).

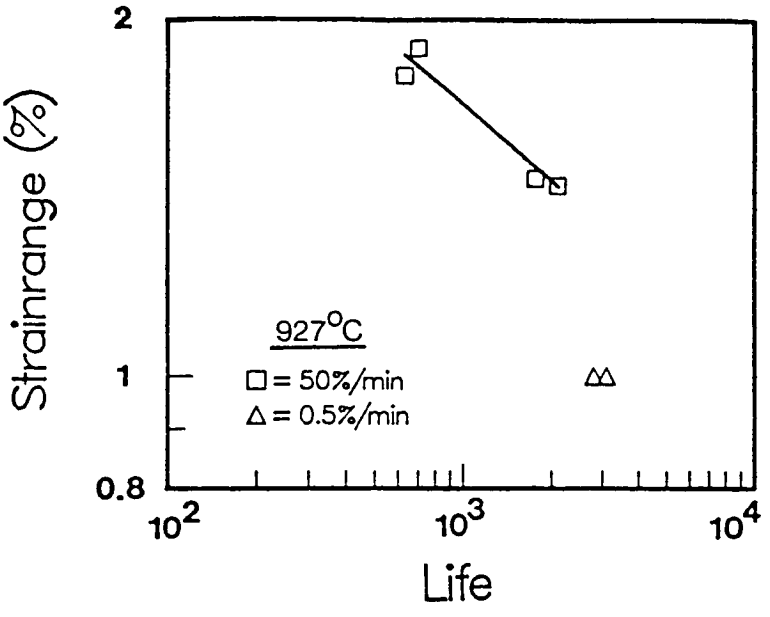

Figure 18. - PWA 1480.

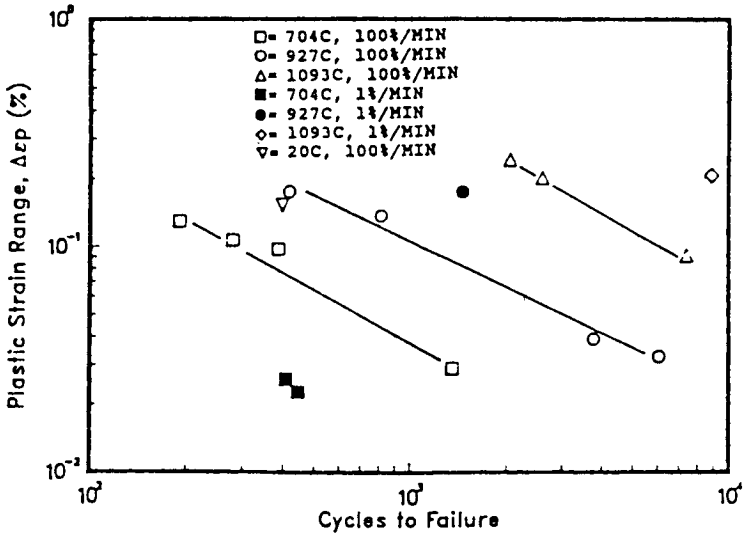

Figure 19. - Mar-M 246.

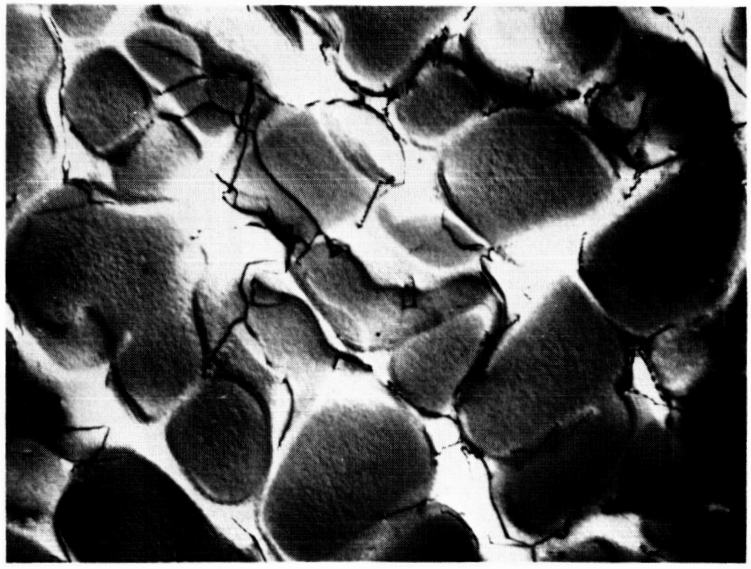

0.5 percent/min

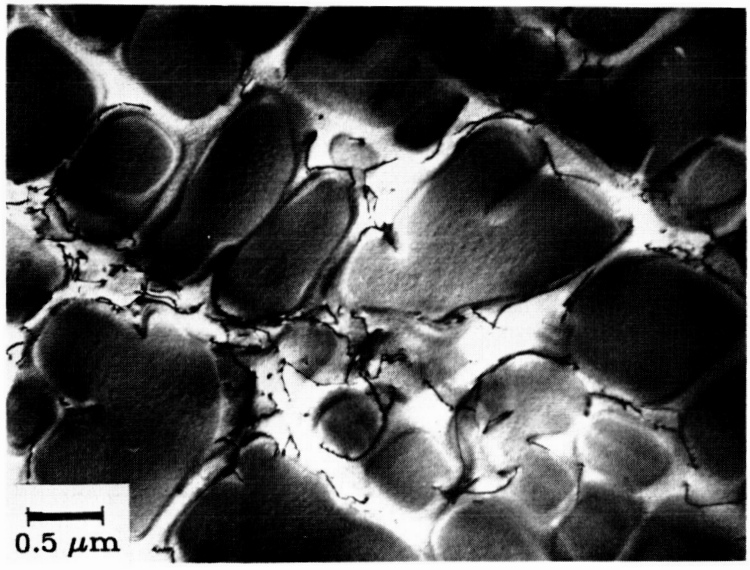

50 percent/min

Figure 20. - 927 °C, $\Delta\varepsilon_p$ = 0.1 percent, N = 4.

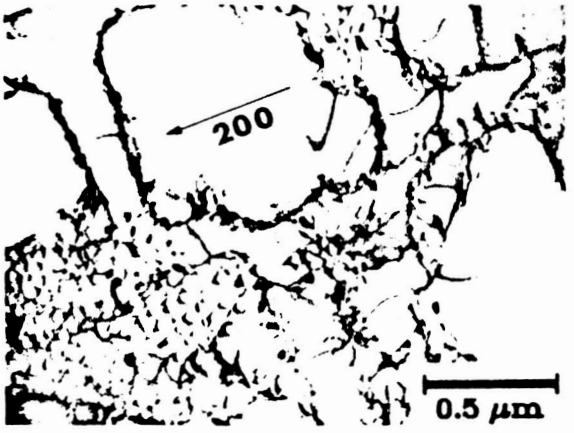

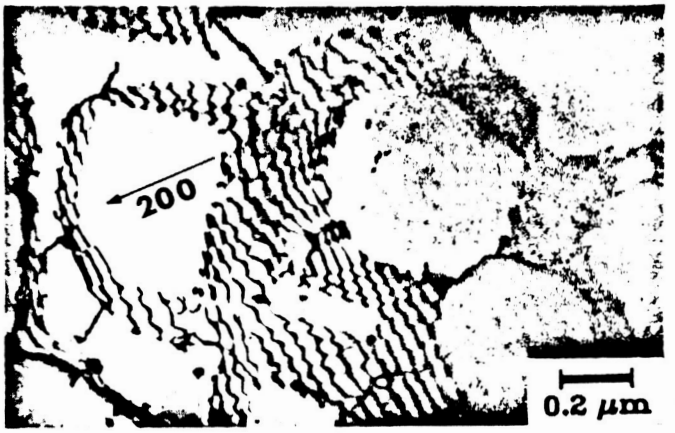

Figure 21. - Mar-M 246 deformation structures after low cycle fatigue at 927 °C.

Original unavailable at time of printing.

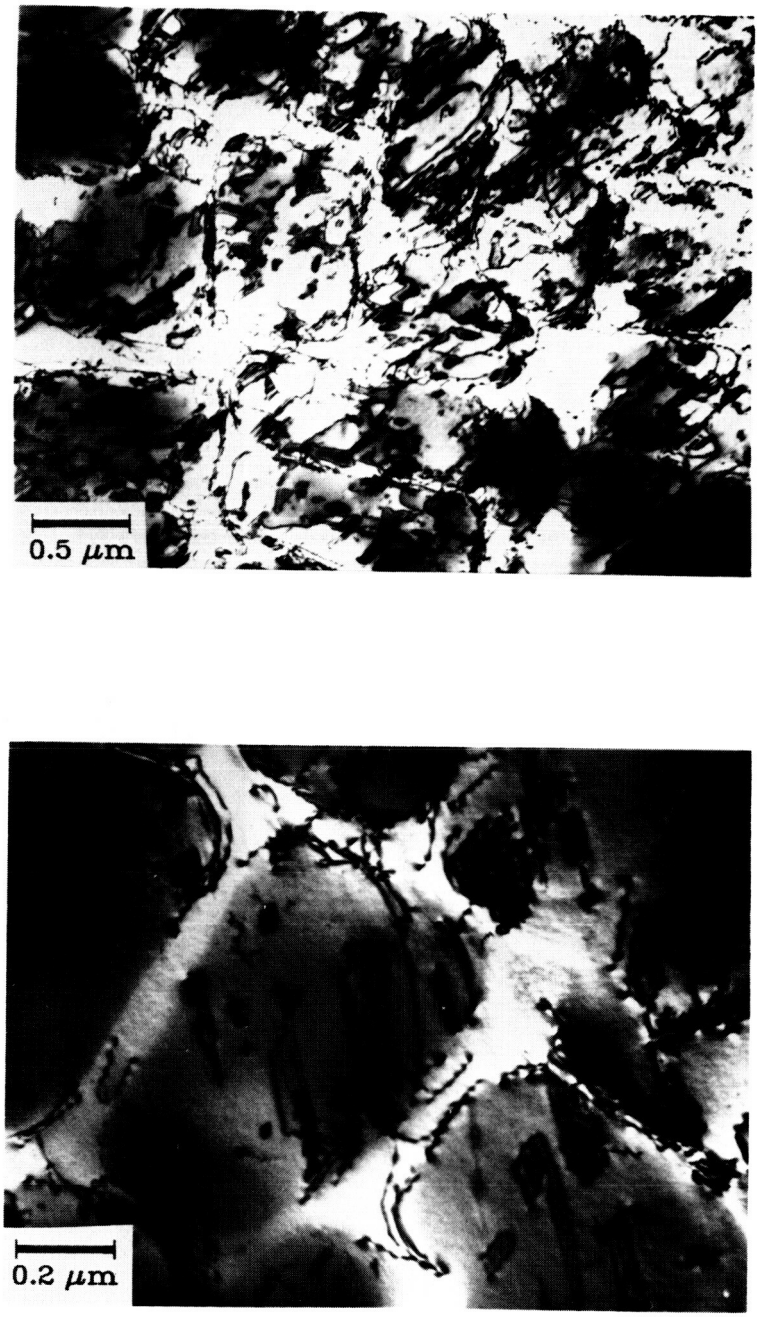

Figure 22. - PWA 1480; 20 °C,
$\Delta\varepsilon_p$ = 0.05 percent, N = 4.

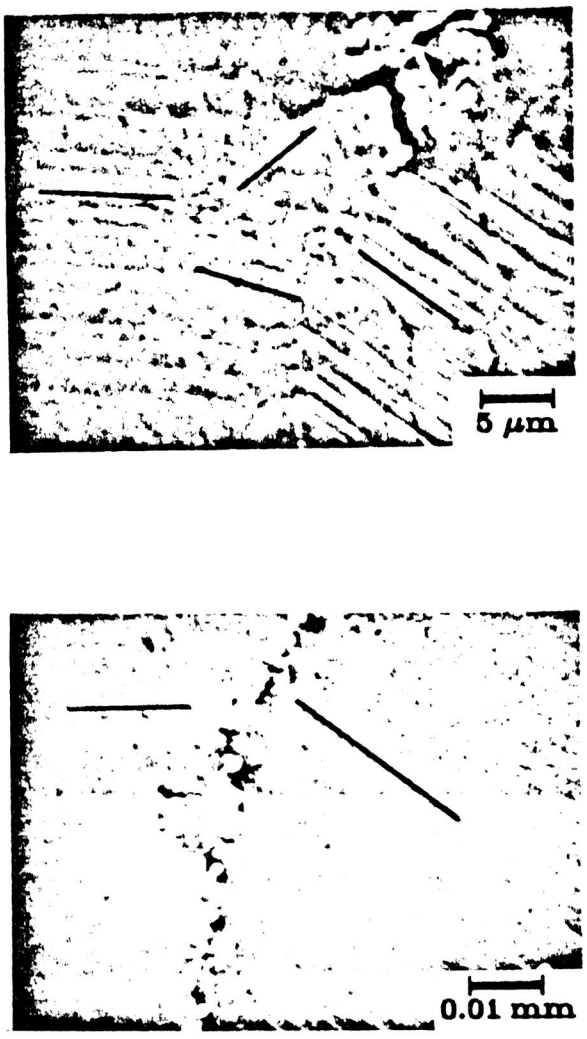

Figure 23. - Surface slip traces after low cycle fatigue at 705 °C, Mar-M 246.

Original unavailable at time of printing.

Deformation during creep,

uniaxial tension and LCF essentially similar

-By-pass at 927 °C

-Shearing at Lower Temps

Figure 24.

Implications

-Unified models justified

-No shearing in (001) crystals at 927 °C

-(123) tests to come

Figure 25.